Constrained Neuro-Identifier for Controlling the Unicycle Mobile Robot

1st Iván Salgado
Medical Robotics and Biosignal Lab
Instituto Politécnico Nacional
Mexico City, Mexico
0000-0002-3854-7031

2nd Manuel Mera
ESIME Ticomán
Instituto Politécnico Nacional
Mexico City, Mexico
0000-0002-9167-9084

3rd Héctor Ríos
Tecnológico Nacional de México
I.T. La Laguna
Coahuila, México
0000-0002-7169-9950

4rd Mariana Ballesteros
Medical Robotics and Biosignal Lab
Mexico, City, Mexico
0000-0003-2879-4474

Abstract—This work proposes the design of a robust controller for the perturbed kinematic model of the unicycle mobile robot, considering a neuro-identifier that imposes restrictions on the identification error. The controller is based on integral sliding modes (ISMs) and the approximation provided by a differential neural network (DNN) for the tracking error dynamics, represented as an uncertain time-varying linear system. The methodology ensures asymptotic stability for the tracking error despite multiplicative disturbances in the control channel. The ISM compensates for the matched dynamics identified with the DNN. Then, a feedback controller based on a Barrier Lyapunov function minimizes the effect of unmatched dynamics while fulfilling state restrictions by solving a set of Linear Matrix Inequalities. Simulation results show the feasibility of the proposed strategy against classical controllers.

Index Terms—Differential Neural Networks, Integral Sliding Modes, Attractive Ellipsoid Method, Barrier Lyapunov Functions

I. Introduction

A. Preliminaries

Various engineering applications require autonomous mobile robots (MRs) to solve particular tasks [1], [2]. For example, in agriculture, using mobile devices allows the identification of pests by monitoring greenhouses and plantations through terrestrial and aerial mobile robotic systems. Consequently, the design of control algorithms allows trajectory tracking, point-to-point movement, or control from a reference model. One of the main challenges involved in creating control techniques for MR is the presence of non-holonomic constraints that limit the use of conventional methods such as linear controllers [3].

Different MRs require a particular analysis to develop control algorithms according to their kinematic configuration. One of the most studied MRs, due to its versatility and freedom of movement, is the Unicycle Robot (UMR), whose

application in real problems is varied [2]. It is important to note that static algorithms cannot stabilize the UMR, based on the Brockett condition [4]. Consequently, most control algorithms implement time-varying feedback control strategies or control algorithms with variable structures that bring robustness against matched perturbations. Many of these developments consider the kinematic, which does not include external forces such as gravity and/or friction in the wheels [5]. However, other phenomena such as skid, slippage, and noise coupled to the control signal must be considered to obtain a robust algorithm for good MRs performance in real applications [6].

Some developments for the control of the UMR implement artificial intelligence such as fuzzy logic [7] or neural networks to produce a time-varying input signal that guarantees the closed-loop stability of the error [8]. Other non-linear techniques consider discontinuous signals to achieve zero tracking error in finite time despite the external uncertainties [6] and [9]. ISMC allows the rejection of disturbances in the control channel and the establishment of nominal control. Composite strategies with high-order sliding modes, discontinuous controls, and feedback techniques have been proposed based on the so-called ellipsoidal methods [10].

In the case of multiplicative disturbances in the control channel, the dynamics can be represented as an uncertain time-varying system. DNNs allow the identification of partially or entirely unknown nonlinear systems. Unlike static networks, the main advantage of these systems are the adaptation laws of the network from controlled Lyapunov functions, guaranteeing practical stability, which is a consequence of the finite number of elements in the approximation base [11]. This approximation error can be rejected by robust techniques based on sliding modes.

B. Contributions

This article proposes a solution to the tracking trajectory problem of a UMR with disturbances in the control channel. The tracking error dynamics represented by an uncertain time-varying system will be identified by the DNN whose stability

is studied through a Barrier Lyapunov function. The DNN identifier restricts the value of the identification error to be rejected later with the ISMC.

C. Notation

The following notation is used throughout the document; the trigonometric functions are denoted as $\mathrm{s}(\theta) = \sin(\theta)$, $\mathrm{c}(\theta) = \cos(\theta)$, $\mathrm{t}(\theta) = \tan(\theta)$, $\mathrm{sc} = \frac{\sin\theta}{\theta}$, $\|\varphi\|_\Lambda^2$ is the weighted norm with $\Lambda_\lambda^\top > 0$, i.e., $\|\varphi\|_\Lambda^2 = \varphi^\top \Lambda \varphi$, I_n is the identity matrix with dimension $n \times n$.

II. PROBLEM STATEMENT

The kinematic model of UMR showed in figure 1 is given by the following set of nonlinear ordinary differential equations

$$
\begin{aligned}
\dot\theta &= [1 + d_1(t)]\omega, \\
\dot x &= [1 + d_2(t)]\mathrm{c}(\theta)v, \\
\dot y &= [1 + d_2(t)]\mathrm{s}(\theta)v,
\end{aligned}
\tag{1}
$$

where $x \in \mathbb{R}$ and $y \in \mathbb{R}$ denote the midpoint between the wheels and $\theta \in \mathbb{R}$ represents the orientation angle of the UMR. $v \in \mathbb{R}$ and $\omega \in \mathbb{R}$ are the linear and angular velocities of the UMR, respectively. These variables constitute the control inputs of the system. The terms of d_1 and d_2 can contain time-varying perturbations, which are multiplicative to the inputs and may come from the commands given to the controllers when executing a control task or non-modeled kinematics proportional to the control inputs. Some examples are the skidding and slippage of the wheels (For more details, see [12], [13]). The following assumptions is fulfilled in this manuscript.

Assumption 1: The time-varying perturbations d_1 and d_2 are unknown but bounded, i.e.,

$$
-1 < d_i(t) \le d_{\max} < 1, \qquad i = 1, 2
\tag{2}
$$

The constraint $d_i \ge -1$, $\forall t \ge 0$ avoids any change of the sign in the control input.

The **problem statement** is to design an ISMC that compensates the estimated unknown dynamics through a Barrier DNN identifier.

III. ROBUST CONTROL DESIGN

A. Time-varying tracking error dynamics

The reference model is given by the following set of ordinary differential equations

$$
\begin{aligned}
\dot\theta_d &= \omega_d, \\
\dot x_d &= \mathrm{c}(\theta_d)v_d, \\
\dot y_d &= \mathrm{s}(\theta_d)v_d,
\end{aligned}
\tag{3}
$$

where x_d, y_d are the UMR desired positions in the $X - Y$ plane, θ_d is the desired angular position, and, v_d and ω_d are the linear and angular reference velocities.

Assumption 2: The desired velocities are continuous and bounded, i.e., $\overline{v}_d$ y $\overline{\omega}_d$, i.e., $0 < \underline{v}_d < v_d(t) \le \overline{v}_d$, y $\|\omega_d\|_\infty \le \overline{\omega}_d$, tal que $v_d(t) \in \mathbb{V} \subset \mathbb{R}$ and $\omega_d(t) \in \mathbb{W} \subset \mathbb{R}$, for all $t \ge 0$.
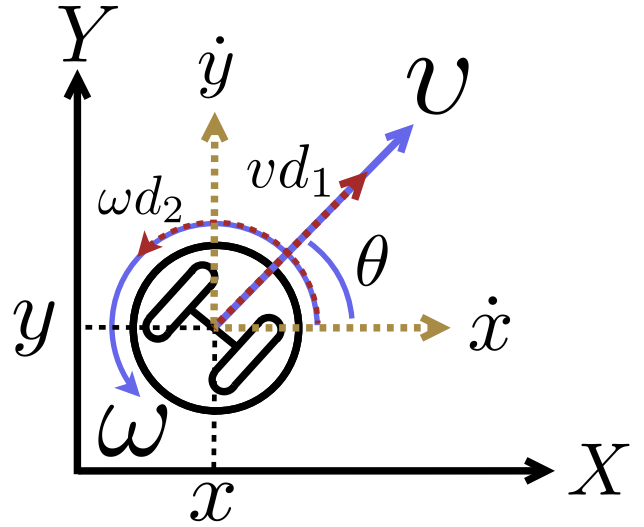

Fig. 1. Robot tipo uniciclo (UMR)

Similarly, $x_d \in \mathbb{X} \subset \mathbb{R}$ and $y_d \in \mathbb{Y} \subset \mathbb{R}$, for all $t \ge 0$. Here, the subsets $\mathbb{V}$, $\mathbb{W}$, $\mathbb{X}$ and $\mathbb{Y}$ contains the admissible inputs and feasible trajectories.

The tracking error is defined as

$$
\begin{aligned}
e_1 &= \theta_d - \theta, \\
e_2 &= \mathrm{c}(\theta)(x_d - x) + \mathrm{s}(\theta)(y_d - y), \\
e_3 &= \mathrm{c}(\theta)(y_d - y) - \mathrm{s}(\theta)(x_d - x),
\end{aligned}
\tag{4}
$$

and, based on (1) and the reference system (3) the dynamics of the tracking error becomes

$$
\begin{aligned}
\dot e_1 &= -\omega d_1(t) + \tau_1, \\
\dot e_2 &= [1 + d_1(t)]\omega e_3 - v d_2(t) + \tau_2, \\
\dot e_3 &= -[1 + d_1(t)]\omega e_2 + v_d \mathrm{s}(e_1),
\end{aligned}
\tag{5}
$$

where the virtual control inputs τ_1 and τ_2 are defined as

$$
\begin{aligned}
\tau_1 &= \omega_d - \omega, \\
\tau_2 &= v_d \mathrm{c}(e_1) - v.
\end{aligned}
\tag{6}
$$

Notice that (5) can be described as a linear parameter varying linear system, i.e.,

$$
\dot e = A(\rho)e + B[\tau + F(\rho)d],
\tag{7}
$$

where $e = (e_1, e_2, e_3)^\top \in \mathbb{R}^3$, $\tau = (\tau_1, \tau_2)^\top \in \mathbb{R}^2$, $d = (d_1, d_2)^\top \in \mathbb{R}^2$. Matrices $A(\rho)$, B y $F(\rho)$ have the following definition

$$
A(\rho) = \begin{pmatrix} 0 & 0 & 0 \\ 0 & 0 & [1 + d_1(t)]\omega \\ v_d \mathrm{sc}(e_1) & -[1 + d_1(t)]\omega & 0 \end{pmatrix},
$$

$$
B = \begin{pmatrix} 1 & 0 \\ 0 & 1 \\ 0 & 0 \end{pmatrix}, \quad F(\rho) = \begin{pmatrix} 0 & -\omega \\ -v & 0 \end{pmatrix},
\tag{8}
$$

The vector $\rho = (v_d \mathrm{sc}(e_1), [1 + d_1(t)]\omega)^\top \in \mathbb{R}^2$ the vector of scheduling variables, which considers the parametric

uncertainties to be identified by the DNN. The control signal is defined as

$$\tau = u_0 + u_1. \tag{9}$$

Based on the work described in [14], the control input (9) has two main components: a discontinuous element u_1 based on SM to compensate matched perturbations, and the nominal controller u_0 composed of a feedback controller and the estimation obtained with the DNN.

B. Constrained non-parametric modeling of the tracking error

Let us assume that the tracking error in (7) is approximated by a DNN with the following structure

$$\dot{e} = (A_0 + W_1^* \sigma_1(e)) \, e + B \, (\tau + W_2^* \sigma_2(e)) + \tilde{f}(e, \rho, d), \tag{10}$$

where $A_0 \in \mathbb{R}^{3 \times 3}$ is a Hurwitz matrix, $W_1^* \in \mathbb{R}^{3 \times 3}$ $W_2^* \in \mathbb{R}^{2 \times 2}$ are the weights that best approximate (in some sense) the uncertain model. These values are unknown but bounded, i.e., $\|W_i^*\|_F^2 \leq W_i^+$, i.e., any quadratic matrix norm with $i = 1, 2$. $\sigma_1 \colon \mathbb{R}^3 \to \mathbb{R}^{3 \times 3}$ and $\sigma_2 \colon \mathbb{R}^3 \to \mathbb{R}^2$ are the activation functions of the DNN selected as sigmoid functions, i.e., each entry of σ_i is described as

$$\sigma_z(e) = \left(a_z + b_z \exp^{-\left(c_z^\top e \right)} \right)^{-1}, \tag{11}$$

where $a_z \in \mathbb{R}$, $b_z \in \mathbb{R}$ and $c_z \in \mathbb{R}^3$ are free parameters defined by the user. With this selection, σ_i with $i = 1, 2$ satisfies the following sector conditions

$$\|\sigma_i(z_2) - \sigma_i(z_1)\|^2 \leq L_{\sigma_i} \|z_2 - z_1\|^2, \quad \forall z_i \in \mathbb{R}^3, \tag{12}$$

moreover, $\|\sigma_i\|^2 \leq \sigma_i^+$.

The unknown function $\tilde{f} \colon \mathbb{R}^3 \times \mathbb{R}^5 \times \mathbb{R}^2 \to \mathbb{R}^3$ includes the unmodeling dynamics, the uncertainties presented in the mathematical model, and the approximation error, i.e., $\tilde{f} = B\tilde{f}_1 + \tilde{f}_2$. The approximation error depends on the sigmoid basis of approximation that contains a finite number of elements [15]. The dynamics of $\tilde{f}$ satisfies the following assumption

Assumption 3: $\tilde{f}$ is bounded as $\|\tilde{f}\|_\Lambda^2 \leq f^+$, with $\Lambda = \Lambda^\top > 0$ being a positive definite matrix.

The DNN identifier is a copy of system (10), i.e.,

$$\dot{\hat{e}} = (A_0 + W(t)\sigma(e))\hat{e} + B \, (\tau + W_2(t)\sigma_2(e)) \,. \tag{13}$$

The learning laws for the identifier are defined as

$$\begin{aligned} \dot{W}_1 &= -\alpha W_1 - K_1 \frac{P\Delta\hat{e}^\top \sigma_1^\top(e)}{\Gamma}, \\ \dot{W}_2 &= -\alpha W_2 - K_2 \frac{B^\top P\Delta\sigma_2^\top(e)}{\Gamma}, \\ \Gamma &= \Delta^+ - \|\Delta\|_P^2 \end{aligned} \tag{14}$$

where $\Delta = \hat{e} - e$ is the identification error, Δ^+ is the bound for the Barrier function (to be defined below), K_1 and K_2 are positive definite matrices of appropriate dimensions known as the learning coefficients of the DNN, $P = P^\top > 0$ is

a positive definite matrix solution of the following matrix (Riccati-like) inequality:

$$\begin{aligned} PA + A^\top P + PRP + \alpha P + Q &\leq 0, \\ R = (W_1^+ + W_2^+)I_{3 \times 3}, & \tag{15} \\ Q = (\sigma_1^+ + L_{\sigma_2^+})I_{3 \times 3}, \qquad \alpha &\in \mathbb{R}_+. \end{aligned}$$

The convergence of the DNN is given in the following theorem.

Theorem 1: Let us consider the tracking error in (7) approximated by the DNN defined in (10) and the identifier proposed in (13) trained with the learning laws in (14). If the matrix inequality in (15) is feasible for a matrix $P = P^\top > 0$, the identification error Δ converges to the set defined by

$$\mathcal{B} \leq \frac{\beta}{\alpha}, \tag{16}$$

with $\beta := W_1^+ + W_2^+ + f^+$ and α being a positive scalar.

Proof: The proof is omitted due to space constraints. ∎

C. Integral sliding mode controller

The DNN identifier can be represented as (the time and variable dependence are omitted in the rest of the manuscript)

$$\dot{\hat{e}} = A\hat{e} + \phi_1 + B \left(\phi_2 + \tau + \tilde{f}_1 \right) + \tilde{f}_2 \tag{17}$$

where ϕ_1 and ϕ_2 are the unmatched and matched dynamics, respectively, of the approximation provided by the DNN. They are defined as $\phi_1 = B^\perp \left(B^\perp \right)^+ W_1 \sigma(e)\hat{e}$ and, $\phi_2 = B^+ W_1 \sigma(e)\hat{e} + W_2 \sigma_2$. Notice that, according to [14], $I_n = BB^+ + B^\perp \left(B^\perp \right)^+$. The terms $\tilde{f}_1$ and $\tilde{f}_2$ consider the modeling and transient identification errors while Δ converges.

Assumption 4: The dynamics of $\tilde{f}_2$ are vanishing, i.e.,

$$\|\tilde{f}_2\|_{Q_{\tilde{f}_2}} \leq \hat{e}^\top Q_{2_e} \hat{e}. \tag{18}$$

With the definition of (9), the nominal control u_0 is selected as

$$u_0 = K\hat{e}, \tag{19}$$

where $K \in \mathbb{R}^{2 \times 3}$ is a gain to be designed below. The robust controller u_1 is based on ISMC, and it is described as

$$u_1 = -\phi_2 - \rho \frac{(GB)^\top s}{\|(GB)^\top s\|}. \tag{20}$$

The gain ρ is a positive constant that must overcome the uncertainties. $s \colon \mathbb{R}^3 \to \mathbb{R}^2$ is the sliding surface defined as

$$\begin{aligned} s(\hat{e}) = G \, (\hat{e}(t) - \hat{e}(0)) - G \int_0^t (A_0\hat{e}(\varphi) + Bu_0(\varphi) \\ + \phi_1(\varphi)) \, d\varphi \end{aligned} \tag{21}$$

D. Main Result

The following theorem describes the main result formulated in this manuscript,

Theorem 2: Let us assume that the tracking error dynamics in (5) is approximated by the BDNN identifier in (13). If the matrix inequality $\Omega \leq 0$ with Ω as

$$\Omega = \begin{pmatrix} P_2 A_0 + A_0^\top P_2 + BK + K^\top B^\top + Q_e + \mu P_2 & P_2 \\ P_2 & -Q_\Phi \end{pmatrix}$$

with Q_Φ a positive definite matrix, is feasible for a matrix $P_2 = P_2^\top \geq 0$ and the control τ (9) is implemented with the nominal control u_0 in (19) with the gain K obtained from (2) and u_1 selected as (20) with $\rho = \|\tilde{f}_1 - (GB)^{-1}G\tilde{f}_2\| + \gamma$ and $\gamma > 0$. The tracking error e in (5) has an stable equilibrium point at the origin.

Proof: The time derivative of the sliding surface in (20) is

$$\dot{s} = GB\left(-\rho \frac{(GB)^\top s}{\|(GB)^\top s\|} + \tilde{f}_1\right) + G\tilde{f}_2. \quad (22)$$

Proposing the Lyapunov function $V_s = s^\top s/2$, with time derivative along the trajectories of the tracking error implementing the control (20) is

$$\dot{V}_s \leq -\|(GB)^\top\|\left(\rho - \|\tilde{f}_1 - (GB)^{-1}G\tilde{f}_2\|\right). \quad (23)$$

Selecting ρ as in Theorem 2, it is possible to guarantee the existence of the sliding mode, i.e.,

$$\dot{V}_s \leq -\gamma \|(GB)^\top\| V_s^{\frac{1}{2}}.$$

In the sliding surface, the equivalent control is defined as

$$v_{D_{eq}} = -(GB)^{-1}G\tilde{f}_2 - \tilde{f}_1, \quad (24)$$

therefore, the tracking error dynamics in the sliding surface becomes

$$\dot{\hat{e}} = A_0\hat{e} + Bu_0 + \Phi, \quad (25)$$

where Φ includes the unmatched perturbation ϕ_1 and the DNN dynamics that can not be compensated directly by the controller, i.e.,

$$\Phi = \phi_1 + \left(I_3 - B(GB)^{-1}G\right)\tilde{f}_2. \quad (26)$$

Based on Assumption 4, Φ is a vanishing term, i.e., $\|\Phi\|_{Q_\Phi} \leq \hat{e}^\top Q_e \hat{e}$. Defining the candidate Lyapunov function $V_2 = \hat{e}^\top P_2 \hat{e}$, with its time-derivative given as $\dot{V}_2 = 2\hat{e}^\top P_2 \dot{\hat{e}}$, and substituting the tracking error dynamics, the following equation is obtained

$$\dot{V} = 2\hat{e}^\top P_2 \left(A_0\hat{e} + Bu_0 + \Phi\right), \quad (27)$$

with the nominal controller u_0, and adding and subtracting the term $\|\Phi\|_{Q_\Phi}$, one has,

$$\dot{V} = \hat{e}^\top \begin{pmatrix} P_2 A_0 + A_0^\top P_2 + BK + K^\top B^\top & P_2 \\ P_2 & -Q_\Phi \end{pmatrix} \hat{e} \\ - \Phi^\top Q_\Phi \Phi. \quad (28)$$

Taking the upperbound of Φ and adding and subtracting $\mu\|\hat{e}\|_{P_2}^2$, it is possible to have the following equation

$$\dot{V} = \hat{e}^\top \Omega \hat{e} - \mu \hat{e}^\top P_2 \hat{e}, \quad (29)$$

with Ω already defined in Theorem 2. If $\Omega \leq 0$, $\dot{V} \leq -\mu V$, this result implies exponential convergence of the tracking error to the origin. ∎

IV. SIMULATION RESULTS

This section shows the feasibility of implementing the proposed control. The reference trajectory used in simulation is $x_d = \cos(w_0 t)$ and $y_d = \sin(2w_0 t)$ with $w_0 = 0.2094$. Then, the desired velocities are given by $\omega_d(t) = (\dot{x}_d\ddot{y}_d - \dot{y}_d\ddot{x}_d)/(\dot{x}_d^2 + \dot{y}_d^2)$ and $v_d(t) = \sqrt{\dot{x}_d^2 + \dot{y}_d^2}$, and $\theta_d(t) = \int_0^t \omega_d(\tau)d\tau$. The value of the disturbances was selected as $d_1(t) = 0.5\sin(3t) + 0.3$ and $d_2(t) = 0.5\cos(t) + 0.3$. All the simulations were carried out with a fourth-order integration method with a sampled period of 0.001 seconds. The initial conditions of the UMR are $x(0) = 1.01$, $y(0) = 0$ and $\theta(0) = 1.5$.

A. Identificador por DNNs

The parameters of the identifier were selected as

$$A_0 = \begin{pmatrix} -10 & 0 & 0 \\ 0 & -10 & 0 \\ 0.1833 & 0 & -10 \end{pmatrix},$$

$$P = \begin{pmatrix} 280 & 0 & 0 \\ 0 & 280 & 0 \\ 0 & 0 & 280 \end{pmatrix}.$$

The learning coefficients were $K_1 = 10.5I_3$ and $K_2 = 10.7I_2$. Regarding the activation functions, σ_1 $q = 3$ was selected as $\sigma_1 = \left[\sigma_{1_{ij}}\right]_{i=1:3,j=1:3}$ with the following elements (according to the definition e proposed in (11)):

$$a_{\sigma_1} = 150\tilde{a}$$
$$\tilde{a} = \begin{pmatrix} 0.5 & 0.7 & -0.2 & 1 & 0.5 & 0.7 & -0.2 & 1 & 02 \end{pmatrix}^\top,$$
$$b_{\sigma_1} = 20\tilde{b}$$
$$\tilde{b} = \begin{pmatrix} 1.5 & 1.7 & 1.2 & 1 & 2.3 & -1.2 & 2.2 & 0.9 & 0.1 \end{pmatrix}^\top,$$
$$c_{\sigma_1} = 20 \times \begin{pmatrix} 0.5470 & 0.1890 & 0.3685 \\ 0.2963 & 0.6868 & 0.6256 \\ 0.7447 & 0.1835 & 0.7802 \end{pmatrix}.$$

We have the following definition for the second set of sigmoidal functions $\sigma_2 = \begin{pmatrix} \sigma_{2_1} & \sigma_{2_2} \end{pmatrix}^\top$ with the following parameters

$$a_{\sigma_2} = 15 \times \begin{pmatrix} 0.5 & 0.7 \end{pmatrix}^\top, \qquad b_{\sigma_2} = 50 \times \begin{pmatrix} 1.5 & 1.7 \end{pmatrix}^\top,$$
$$c_{\sigma_2} = 5 \times \begin{pmatrix} 0.5470 & 0.1890 & 0.3685 \\ 0.5470 & 0.1890 & 0.3685 \end{pmatrix}.$$

The initial conditions of the weights (W_1, W_2) were chosen arbitrarly with values between 0 and 1. The initial conditions of the identifier were taken as zero.

Figure 2 shows the tracking error estimation by the identifier. It is important to note that the error trajectories are estimated correctly after the training period. The training
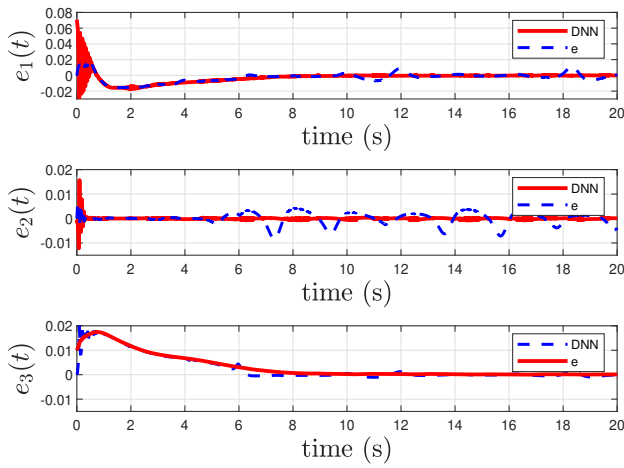
Fig. 2. DNN tracking error estimation The dotted blue line represents the real trajectories and the solid red line represents trajectories generated by the DNN.
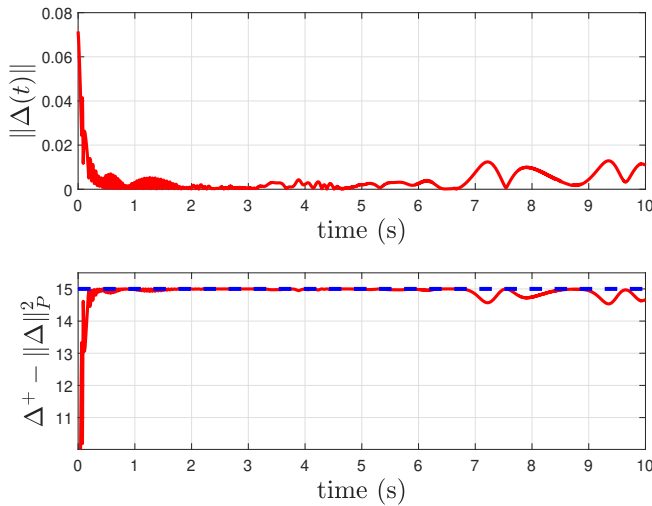

Fig. 3. Euclidean norm of the tracking error. Only the first 10 seconds of the simulation are plotted, which is the time it takes for the network to identify the error trajectories.

period was less than one second; this allows for compensating the time-varying dynamics of the system through the control composed of ISM and the feedback of states. Figure 3a depicts the norm of the identification error. This metric corroborates the performance of the identifier and the result obtained in Theorem 1, which proves practical stability. For simulation, the above emphasizes the network's learning process, which are the oscillations shown in the first 0.5 seconds of simulation. Once this period passes, the identification error remains close to zero. For the initial condition, the term $\Delta^\top(0)P\Delta(0)$ in Γ shown in equation (14) is equal to 14.3139. Therefore, the bound Δ^+ was selected as 15 in the simulation. In Figure 3, $\Delta^\top P\Delta$ did not grow above the value of Δ^+. This is the effect of the Barrier technique.
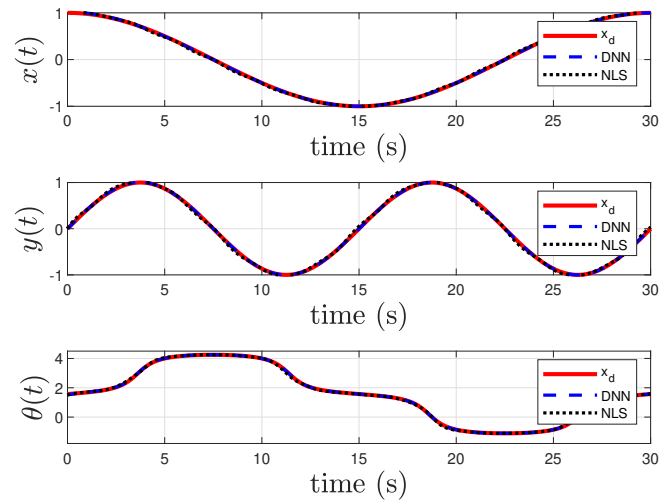

Fig. 4. Comparison of the trajectory tracking of the UMR by the ISMC compensating for the non-linearities coupled to the control using the DNN-based identifier.

B. Integral sliding mode control

The control parameters by ISM were selected as $G = B^+$, $\gamma = 0.75$. The gain for nominal control u_0 was obtained as

$$K = \begin{pmatrix} 1.75 & 0 & 3.4097 \\ 0 & 1.55 & 0 \end{pmatrix}.$$

The proposed controller in this work was compared with the strategy presented in [16], that is,

$$v = v_d(t)\cos(e_1) + K_x e_2,$$

$$\omega = \omega_d + K_\theta e_1 + v_d K_y e_2 \phi(e_1), \tag{30}$$

$$\phi(e_1) = \frac{\sin(e_1)}{4} e_1.$$

The values used in the simulation were $K_x = K_y = K_\theta = 4$. Figure (4) shows the trajectory tracking of the UMR. Both controls perform trajectory tracking. However, the presence of the disturbance causes some oscillations with the controller described in (30). Notice the oscillations produced by the multiplicative disturbances $d_1(t)$ and $d_2(t)$. This oscillation is completely attenuated by applying the control based on ISM and DNNs. Figure 5 shows trajectory tracking in the $x - y$ plane. At first glance, it is impossible to appreciate the advantages of the controller by ISMC. Due to the above, figure 6 shows the norm two of the tracking error with both strategies. The solid red line represents the tracking error by applying the DNN, which presents oscillations at the beginning of the simulation corresponding to the training period of the DNN. Later, it converges to a smaller region than the nonlinear controller proposed in the equations (30). This graph demonstrates the advantages of applying the combined algorithm between DNN and ISMC.

V. CONCLUSIONS

The technique applied in this article allows the estimation of the time-variant part of the UMR tracking error using
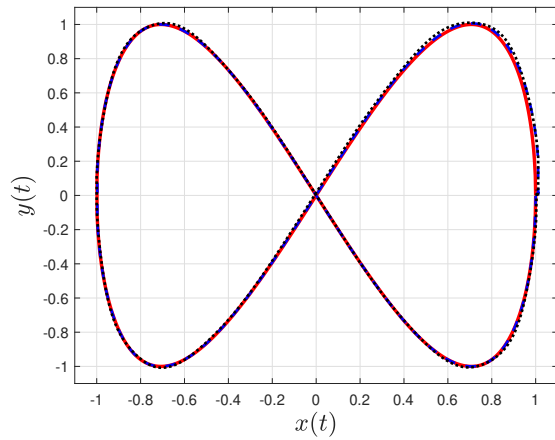
Fig. 5. Phase state diagram in the plane $X - Y$. The red line is the desired trajectory, the blue line is the control compensating with the DNN and ISMC, and the black dotted line is the control in (30)
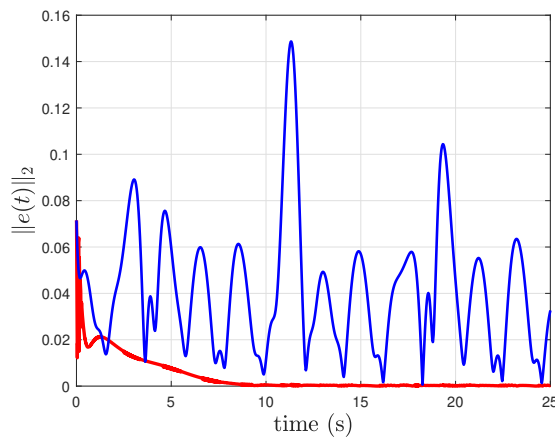

Fig. 6. Euclidean norm of the tracking trajectory error. The blue line represents no linear control in (30), and the red line is the controller given by the DNN and the ISM.

DNNs. The performance is improved with the compensation of the unknown dynamics estimated by the DNNs. As a result, obtaining a smaller convergence zone is possible compared to classical control techniques. The effect of the Barrier DNN did not allow the tracking error to grow above a given condition.

REFERENCES

[1] F. Rubio, F. Valero, and C. Llopis-Albert, "A review of mobile robots: Concepts, methods, theoretical framework, and applications," *International Journal of Advanced Robotic Systems*, vol. 16, no. 2, p. 1729881419839596, 2019.

[2] B. Patle, A. Pandey, D. Parhi, A. Jagadeesh, *et al.*, "A review: On path planning strategies for navigation of mobile robot," *Defence Technology*, vol. 15, no. 4, pp. 582–606, 2019.

[3] B. Hichri, A. Gallala, F. Giovannini, and S. Kedziora, "Mobile robots path planning and mobile multirobots control: A review," *Robotica*, pp. 1–14, 2022.

[4] F. Pourboghrat, "Exponential stabilization of nonholonomic mobile robots," *Computers & Electrical Engineering*, vol. 28, no. 5, pp. 349–359, 2002.

[5] S. G. Tzafestas, "Mobile robot control and navigation: A global overview," *Journal of Intelligent & Robotic Systems*, vol. 91, pp. 35–58, 2018.

[6] P. Rochel, H. Ríos, M. Mera, and A. Dzul, "Trajectory tracking for uncertain unicycle mobile robots: A super-twisting approach," *Control Engineering Practice*, vol. 122, p. 105078, 2022.

[7] T. Das and I. N. Kar, "Design and implementation of an adaptive fuzzy logic-based controller for wheeled mobile robots," *IEEE Transactions on Control Systems Technology*, vol. 14, no. 3, pp. 501–510, 2006.

[8] F. Pourboghrat and M. P. Karlsson, "Adaptive control of dynamic mobile robots with nonholonomic constraints," *Computers & Electrical Engineering*, vol. 28, no. 4, pp. 241–253, 2002.

[9] Y. Díaz, J. Dávila, and M. Mera, "Leader-follower formation of unicycle mobile robots using sliding mode control," *IEEE Control Systems Letters*, vol. 7, pp. 883–888, 2022.

[10] A. Gutiérrez, M. Mera, and H. Ríos, "An integral sliding–mode robust regulation for constrained three–wheeled omnidirectional mobile robots," in *2022 IEEE 61st Conference on Decision and Control (CDC)*, pp. 3637–3642, IEEE, 2022.

[11] A. Poznyak, S. Noriega-Marquez, A. Hernandez-Sanchez, M. Ballesteros-Escamilla, and I. Chairez, "Min–max dynamic programming control for systems with uncertain mathematical models via differential neural network bellman's function approximation," *Mathematics*, vol. 11, no. 5, p. 1211, 2023.

[12] M. Guerra, D. Efimov, G. Zheng, and W. Perruquetti, "Avoiding local minima in the potential field method using input-to-state stability," *Control Engineering Practice*, vol. 55, pp. 174–184, 2016.

[13] D. Wang and C. B. Low, "Modeling and analysis of skidding and slipping in wheeled mobile robots: Control design perspective," *IEEE Transactions on Robotics*, vol. 24, no. 3, pp. 676–687, 2008.

[14] M. Rubagotti, A. Estrada, F. Castaños, A. Ferrara, and L. Fridman, "Integral sliding mode control for nonlinear systems with matched and unmatched perturbations," *IEEE Transactions on Automatic Control*, vol. 56, no. 11, pp. 2699–2704, 2011.

[15] G. Cybenko, "Approximation by superpositions of a sigmoidal function," *Mathematics of Control, Signals and Systems*, vol. 5, pp. 455–455, 1992.

[16] M. Maghenem, A. Loría, and E. Panteley, "Formation-tracking control of autonomous vehicles under relaxed persistency of excitation conditions," *IEEE Transactions on Control Systems Technology*, vol. 26, no. 5, pp. 1860–1865, 2017.